Supporting Information

Kauwe and Isacoff 10.1073/pnas.1221314110

SI Materials and Methods

Electrophysiology. Single electrode current clamp and two-electrode voltage clamp measurements were done with an Axoclamp 2B amplifier (Molecular Devices) on *Drosophila* muscle 6 at segment A3 of third instar larvae. Recording solution was standard haemolymph 3 (HL3), containing in millimoles: 1.5 Ca^{2+}, 70 NaCl, 5 KCl, 20 $CaCl_2$, 20 $MgCl_2$, 10 $NaHCO_3$, 5 trehalose, 115 sucrose, and 5 Hepes. In experiments with light-gated mammalian iGluR6 (LiGluR) activation, we added 2 μM thapsigargin (Calbiochem) and 30 mg/100 mL of Con A (Sigma-Aldrich) to HL3. Recording electrodes contained 3M KCl with resistances in the range 15–25 MΩ. Muscles with a membrane potential below −60 mV and at least 4 MΩ input resistance were chosen for studies. Signals were filtered at 1 KHz and recorded at 5 kHz using a Digidata 1200A/B board and Clampex 8.0 software (Axon Instruments). Miniature synaptic transmission data were analyzed with MiniAnalysis software (Synaptosoft), and evoked synaptic transmission data were analyzed with Clampfit 8.0 (Axon Instruments). dibutyryl (Db)-cAMP (Tocris) (100× stock in water) was used at 1 mM, R-adenosine, cyclic 3′,5′-(hydrogenphosphorothioate) triethylammonium (Rp)-cAMP (Tocris) (1000× stock in water) was used at 100 μM, cytochalasin D (Sigma) (1000× stock in ethanol) was used at 10 μM, and Philanthotoxin-433 (Invitrogen) (1000× stock in DMSO) was used at 4 μM.

Maleimide-Azobenzene-Glutamate Labeling and Optical Stimulation of LiGluR. Third instar larvae were dissected into a fillet in 0.45 mM Ca^{2+} HL3 solution. Fillets were then incubated with the brain intact for 12 min in 1.5 mM Ca^{2+} HL3 with 2 μM thapsigargin and 30 mg/100 mL of Con A. HL3 solution was removed and replaced with 50 μM of maleimide-azobenzene-glutamate (MAG) (kindly provided by Dirk Trauner, University of Munich, Munich, Germany) in 0.45 mM Ca^{2+} HL3 which had been pre-illuminated with 380 nm light for 3 min (1% final DMSO concentration). Fillets were incubated in MAG for 20 min in dark. MAG was removed and fillets were washed two times with 1.5 mM Ca^{2+} HL3. Preparations were illuminated with a Lambda LS 300W Xenon arc lamp system (Sutter) with excitation filters (Chroma) of 380/30 nm to activate LiGluR and 470/40 nm to deactivate it.

Immunohistochemistry. We performed antibody labeling using standard *Drosophila* procedures. Third instar larvae were dissected in 0.45 mM Ca^{2+} HL3 and fixed for 20 min in 3.7% (vol/vol) formaldehyde in PBS or 5 min in Bouin's [glutamate receptor IIA (GluRIIA) antibody]. The following primary antibodies were used: anti-GluR6/7 (1:500; Millipore), anti-GluRIIA [1:100; Developmental Studies Hybridoma Bank (DSHB)], anti-Bruchpilot (Brp) (1:100; DSHB), anti-HRP-Cy3 (1:100; Jackson ImmunoResearch), and anti-Dlg (Discs Large) (1:250; DSHB). The following secondary antibodies were used: anti-rabbit 647 (1:500; Invitrogen) and anti-mouse 532 (1:500; Invitrogen). Images were acquired with the Zeiss LSM 780 in the Molecular Imaging Center at University of California, Berkeley.

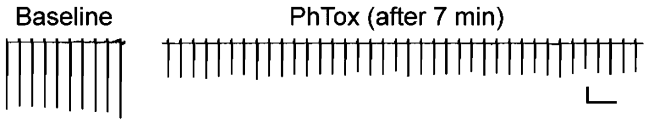

Fig. S1. Stable partial block of native ionotropic glutamate receptors (iGluRs) by philanthotoxin-433 (PhTox). In the standard neuromuscular junction (NMJ) preparation that we used (muscle stretched and voltage clamped), 4 μM PhTox reduced the amplitude of excitatory postsynaptic currents (EPSCs) evoked at 0.1 Hz by ∼50% in wild-type NMJs and this block was stable. (Scale bar: 30 nA and 20 s.)

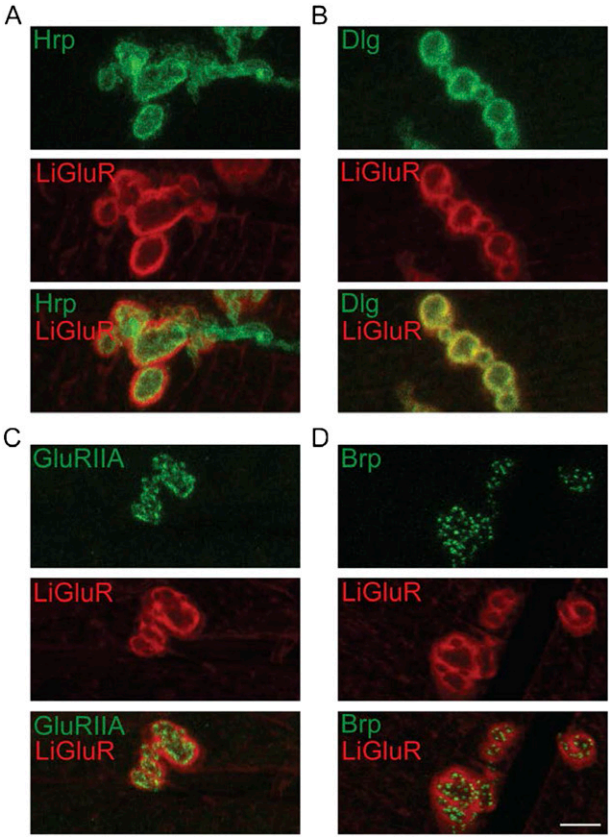

Fig. S2. Postsynaptic localization of LiGluR. (*A–D*) Confocal images compare postsynaptic antibody labeling of LiGluR (red) with antihorseradish peroxidase (HRP) staining of presynaptic nerve terminal (*A*, green), or postsynaptic antibody labeling of Discs Large (Dlg) (*B*, green), or postsynaptic antibody labeling of GluRIIA glutamate receptor subunit (*C*, green), or presynaptic active zone protein Bruchpilot (*D*, green). (Scale bar: 5 μm.) Note that much of LiGluR is extrasynaptic with only a portion overlapping with active zones and *Drosophila* glutamate receptors.

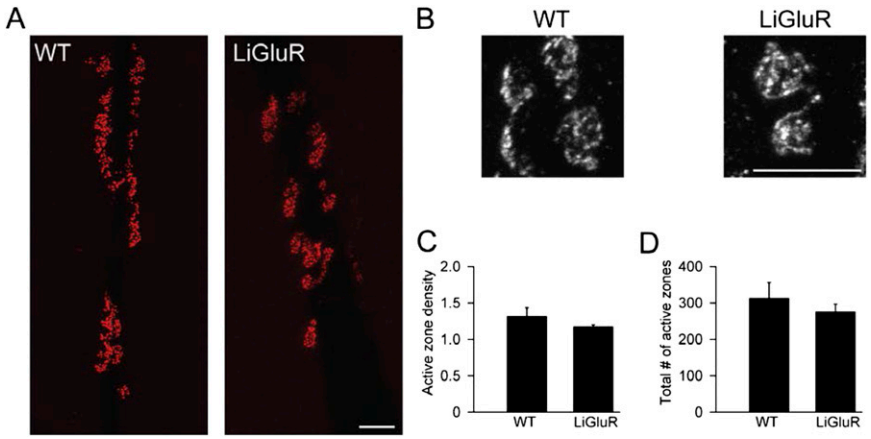

Fig. S3. Postsynaptic LiGluR does not alter Bruchpilot (Brp) or GluRIIA distribution at the NMJ. (*A* and *B*) Representative confocal images show antibody labeling of Brp (*A*) and GluRIIA (*B*) for *w1118* (WT) and LiGluR expressing NMJs. (*C*) Bar graph shows average active zone density (no. of Brp spots per bouton area) between wild type ($n = 5$) and LiGluR-expressing ($n = 5$) NMJs. For each NMJ, the 10 largest boutons were selected and measured for their bouton area and number of Brp spots to generate an average bouton density for each NMJ. (*D*) Bar graph shows average total number of active zones between wild type ($n = 7$) and LiGluR-expressing ($n = 6$) NMJs. Active zone density ($P = 0.236$) and total number of active zones ($P = 0.476$) are not significantly different between the groups based on Student *t* test. (Scale bars: 10 μm.)

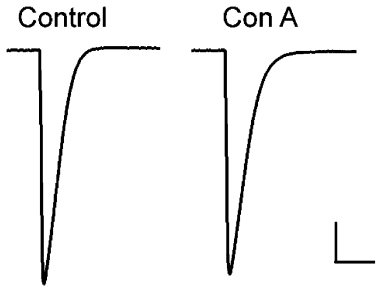

Fig. S4. Con A does not alter EPSC amplitude. EPSCs (average of 10 evoked at 0.1 Hz) from wild-type NMJs without Con A (*Left*) and with Con A (*Right*) in bath solution. (Scale bar: 25 nA and 20 ms.)

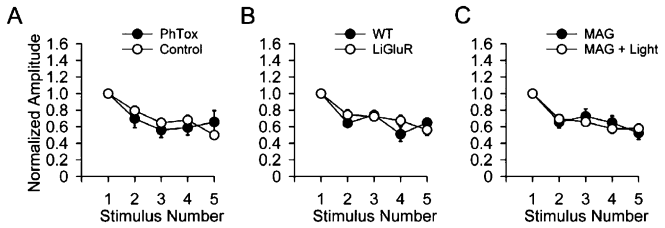

Fig. S5. Intraburst synaptic depression is not affected by block of native GluRs with PhTox or the expression or optical activation of LiGluR. (*A–C*) Average amplitudes of first five EPSCs of eight 20-Hz trains (normalized amplitude of first EPSC in the train). No effect on intraburst depression of: (*A*) PhTox (filled circles, $n = 10$) compared with 0.1% DMSO vehicle control (open circles, $n = 8$) (same NMJs as in Fig. 1); (*B*) LiGluR expression (open circles, $n = 5$) versus wild type (filled circles, $n = 7$) (NMJs treated with thapsigargin, no MAG labeling); and (*C*) LiGluR-expressing NMJs labeled with MAG that are either activated by light (open circles, $n = 13$) or not activated by light (filled circles, $n = 12$) (same NMJs used in Fig. 3).

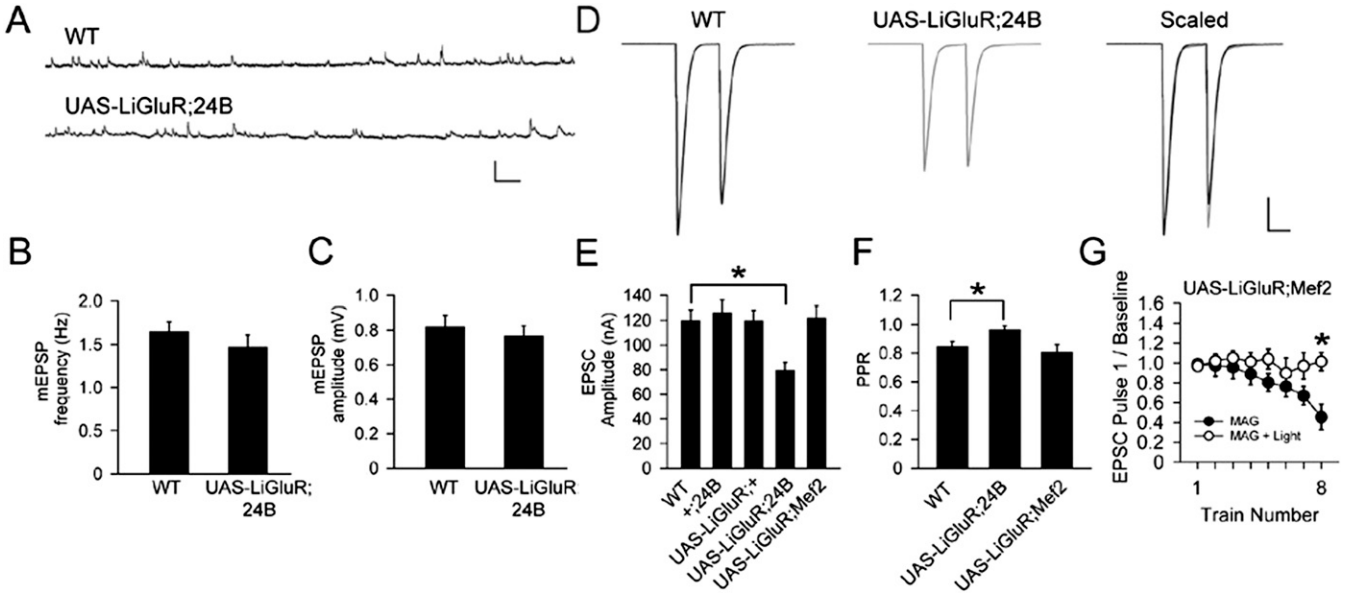

Fig. S6. LiGluR-evoked enhancement of recovery from depression at normal homeostatic set point. (*A–F*) High muscle expression of upstream activating sequence (UAS)-LiGluR driven by yeast GAL4 protein 24B-GAL4 decreases EPSC amplitude with no change in miniature excitatory postsynaptic potential (mEPSP) amplitude and increases paired pulse ratio (PPR), indicating a decrease in quantal content, but weaker expression driven by myocyte enhancer factor-2 GAL4 (Mef2-GAL4) leaves EPSC amplitude and PPR unchanged from wild type, indicating normal quantal content. (*A*) Representative mEPSP traces recorded from WT muscles and UAS-LiGluR; 24B-GAL4 muscles. (*B* and *C*) Averaged mEPSP frequency (*B*) and averaged mEPSP amplitude (*C*) for WT ($n = 11$) and UAS-LiGluR; 24B-GAL4 ($n = 9$). (*D*) Representative paired pulse traces with 50-ms interpulse interval. Scaled traces have first pulse amplitudes matched between WT and LiGluR to visualize difference. (*E*) Average data across all NMJs for single pulse evoked EPSCs for WT ($n = 15$), w; + ;24B ($n = 10$), *w*; UAS-LiGluR; + ($n = 13$), *w*; UAS-LiGluR; 24B ($n = 16$), and *w*; UAS-LiGluR; Mef2 ($n = 10$). Ten pulses at 0.1 Hz were collected and averaged. One-way ANOVA followed by post hoc Scheffé's test. NMJs expressing LiGluR with 24B exhibit a significant decrease in evoked EPSC amplitudes compared with wild type ($P < 0.05$). EPSC amplitudes for NMJs expressing LiGluR with Mef2 are not different from wild type ($P = 0.999$). (*F*) Average paired pulse ratio (PPR) (pulse 2/pulse 1) for WT ($n = 14$), *w*; UAS-LiGluR; 24B ($n = 12$), and *w*; UAS-LiGluR; Mef2 ($n = 6$). PPR for each NMJ is average of calculations from 10 paired pulses at 0.1 Hz. NMJs expressing LiGluR with 24B have a statistically significant increase in PPR compared with wild type ($P < 0.05$). NMJs expressing LiGluR with Mef2 are not significantly different in PPR from wild type ($P = 0.816$) (One-way ANOVA followed by a post hoc Scheffé's test). (*G*) NMJs expressing UAS-LiGluR under Mef2-Gal4 exhibit enhanced recovery from synaptic depression in response to light. Average values of pulse 1 normalized to baseline for trains 1–8 with *w*; UAS-LiGluR; Mef2 in MAG only (no light control) ($n = 5$) and MAG with light ($n = 4$). *$P < 0.05$, Student *t* test. (Scale bar: *A*, 2 mV and 500 ms and *D*, 20 nA and 50 ms.)

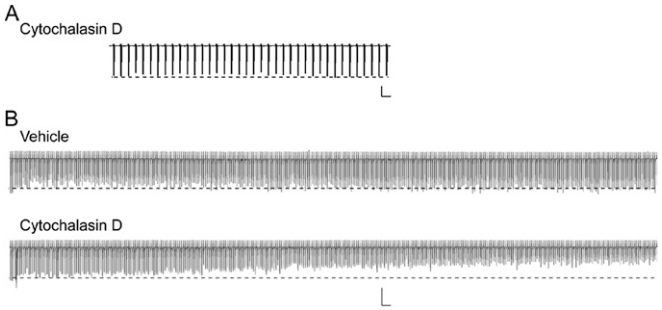

Fig. S7. Cytochalasin D blocks reserve pool recruitment during high-frequency stimulation. (*A*) No synaptic depression during 5 min of continuous 0.1-Hz motor axon stimulation in NMJs expressing LiGluR in muscle 10 min after addition of 10 μM cytochalasin D (in 0.1% ethanol), consistent with sufficient time for vesicle recycling and lack of recruitment of vesicles from the reserve pool at low frequency. (*B*) Substantial synaptic depression during 45 s of continuous 10-Hz motor axon stimulation in NMJs expressing LiGluR in muscle 10 min after addition of 10 μM cytochalasin D (in 0.1% ethanol), but not after addition of vehicle (0.1% ethanol alone), consistent with depletion of readily releasable vesicle pool and recruitment of vesicles from the reserve pool at high frequency. (Scale bar: *A*, 20 nA and 10 s and *B*, 20 nA and 500 ms.)

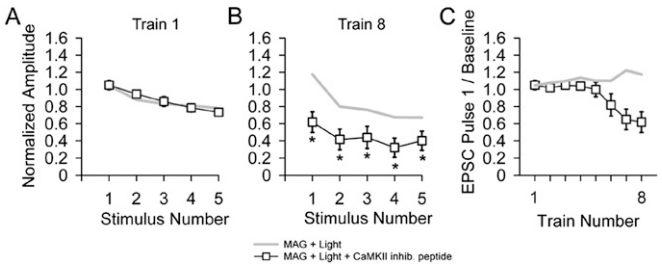

Fig. S8. LiGluR enhancement of recovery from synaptic depression depends on postsynaptic Ca^{2+}/calmodulin-dependent protein kinase II (CaMKII) activity. Averaged first five EPSCs in train 1 (*A*) and train 8 (*B*) and averaged pulse 1 normalized to the baseline across trains 1–8 (*C*) for LiGluR + MAG + light with muscle coexpression of the CaMKII inhibitory peptide (open squares, $n = 8$) or without it (gray line, data from Fig. 3*C*). Muscle expressing the CaMKII inhibitory peptide had significantly greater accumulated depression of the EPSCs (Student *t* test, $P < 0.05$), approximating what was seen in absence of optical stimulation of LiGluR (Fig. 3*C*).